CHAPTER 4

RESULTS AND DISCUSSIONS

4.1 SOLUTION OF THE CONTINUITY EQUATION USING THE FCT ALGORITHM

From the previous discussion, the fluid behavior of the plasma can be represented by the continuity equation. In order to solve this equation, the FCT algorithm is selected. In this section, the performance of the FCT algorithm and especially its accuracy, will be tested.

In this study, comparison is made between two methods of computation. The first method was based on a simple three-point approximation algorithm, and the second method is based on the Phoenical SHASTA, which is one of the versions of the FCT method.

For test comparison, a standard sinusoidal spike pulse is initially assumed to exist near the cathode. This initial pulse is accelerated under a uniform electrical field of E=5kV/cm. Results are generated using three different mesh sizes, i.e., (a) Δx =0.0005cm, (b) Δx =0.001cm, (c) Δx =0.002cm, while Δt is fixed at 0.01nsec. The profile of the pulse is recorded every 2nsec for comparison purpose. The results are shown in Fig(4.1.1) and Fig(4.1.2).

From the results, the pulse profile may change after some period of time of simulation. This is due to the numerical errors of the three-point approximation method that

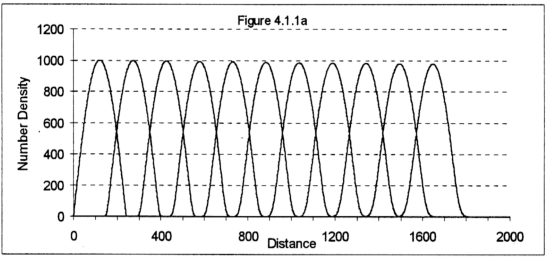

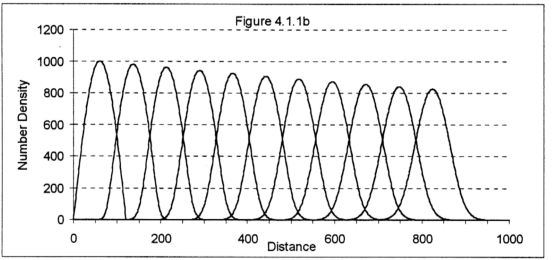

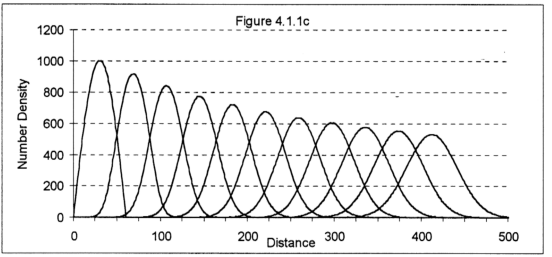

Figure 4.1.1: Simulation Of Sinusoidal Pulse (Non FCT Method)
(a) $\Delta x = 0.0005$cm; (b) $\Delta x = 0.001$cm; (c) $\Delta x = 0.002$cm;

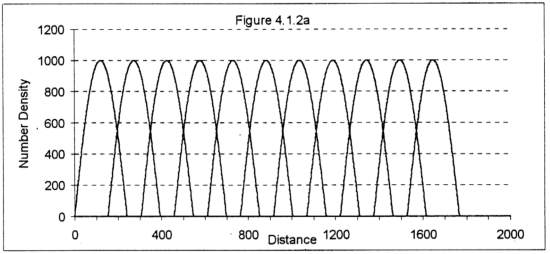

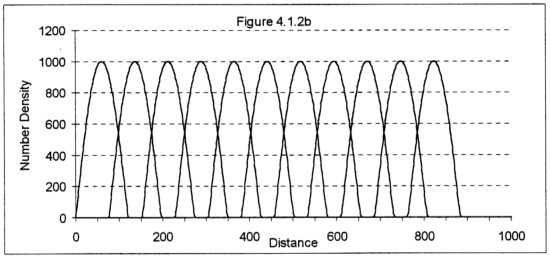

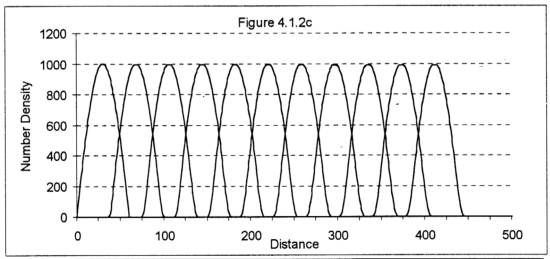

Figure 4.1.2: Simulation Of Sinusoidal Pulse (FCT Method)
(a) $\Delta x = 0.0005$cm; (b) $\Delta x = 0.001$cm; (c) $\Delta x = 0.002$cm;

has been used. From the results shown in Fig(4.1.1), the peak of the pulse will slowly decay and the width of the pulse is broader.

These errors are more apparent if the larger Δx mesh has been used. If Δx is 0.0005cm, the peak of the pulse decays by 2.36%. As Δx gets larger at 0.001cm and 0.002cm, the peak will have percentage errors with 17.51% and 46.88% respectively.

From the discussions above, the ordinary three-point approximation method is not the best choice to simulate the plasma in the discharge, since the space charge effect occurs with a steep gradient. The ordinary algorithm may not handle it well and this will cause some unavoidable errors. Although the numerical error can be reduced by using smaller Δx, it will however increase the computing time.

On the other hand, when compared with the results shown at Fig(4.1.2) using the FCT algorithm, the pulse shape is better preserved under the same conditions. The simulation is within an acceptable level although the simulation is carried out with different Δx. The errors are less than 0.2% for Δx of 0.001cm and less than 0.8% when Δx is 0.002cm. However the best choice of Δx is 0.0005cm where the decay error is below 0.03%. The stability of the FCT algorithm is maintained since the only condition as listed below has been achieved.

$$\left|\frac{\Delta t}{\Delta x}u\right| \leq \frac{1}{2} \qquad 4.1.1$$

This important condition needs to be complied in order to maintain the stability and positivity of the FCT algorithm. Further explanation on this condition has been discussed previously in chapter 2.

As expected (Boris and Book, 1976; Morrow, 1981), the FCT method is able to handle the simulation with a high degree of accuracy while maintaining the stability. This

powerful algorithm is selected as the tool to simulate the plasma with a steep gradient behavior in the next section, since it manages to handle it particularly well.

4.2 THE FLUID EQUATION WITH THE SOURCE TERMS

In order to simulate the Townsend process in the discharge channel, the source term is added into the continuity equation.

Numerical solution of the source term may require a higher order of accuracy in the simulation. From the discussions at section 3.6.2, there are three methods that can be used in order to add the source term to the fluid equation. These are the simple Euler step, single auxiliary step and the double auxiliary step methods.

In this section, the accuracies of using these three methods were tested. Some important assumptions have been made. The integration of the source term is tested under a uniform electrical field and a constant electron density throughout the space. The constant electron density constitutes a large square wave which moves along at velocity u while its top remains flat, so that the diffusion term in Eq(3.6.2) will become:

$$\frac{\partial(nu)}{\partial x} = 0 \qquad 4.2.1$$

And the electron density on the channel increases as the equation below.

$$\frac{\partial n}{\partial t} = S$$

$$= n|u|\alpha \qquad 4.2.2$$

and so the electron density at time t is

$$n_t = n_o \exp(t|u|\alpha) \qquad 4.2.3$$

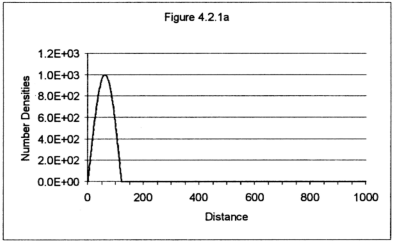

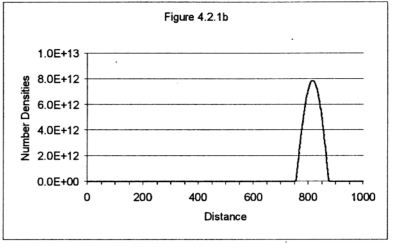

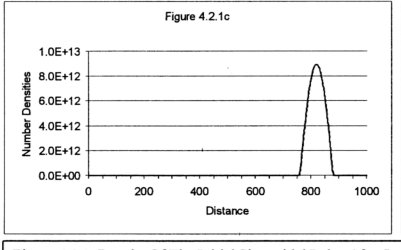

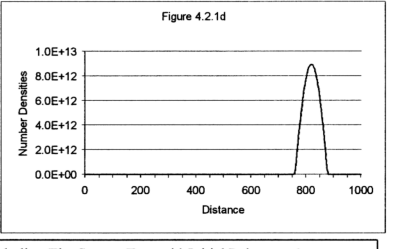

Figure 4.2.1: Results Of The Initial Sinusoidal Pulse After Including The Source Term. (a) Initial Pulse at t=0ns. Simulation with (b) Normal Eulerian Step; (c) Single Auxiliary Step; (d) Double Auxiliary Step at t=20ns.

where t is the elapsed time, n_o is the initial electron density and is taken to be $1000cm^{-3}$ in this test. The applied electrical field is 5kV/cm and the gas pressure is 50mbar. From the calculation by using Eq(4.2.3), the electron density after 20nsec, n_{20} is $8.945\times10^{12}cm^{-3}$.

The first test was carried out by using the normal eulerian step and the result is shown in Fig(4.2.1). This method gives $n_{20} \approx 7.843\times10^{12}$ and the difference is 12.31%. However, when the auxiliary step methods were applied, these differences can be reduced. For the single auxiliary step, the method shows $n_{20} \approx 8.927\times10^{12}$ and the percentage error is 0.19%. However, the double auxiliary step shows $n_{20} \approx 8.930\times10^{12}$ with the percentage error of 0.15%.

From these results, it seems that a proper calculation of the source term can be obtained by applying either of the auxiliary step methods. These two methods can reduce the error percentage within an acceptable level. The integration of the source term should be at least second order in time in order to maintain the stability and accuracy.

4.3 THE CHARACTERISTICS OF THE ELECTRICAL DISCHARGE UNDER UNIFORM ELECTRICAL FIELD SIMULATION

In this section, the electrical discharge of the nitrogen laser will be studied. The results are carried out by the FCT model by assuming the electrical field in the discharge gap is uniformly distributed. Comparisons are also made for this new model and the model of Fitzsimmons, (1976).

In this study, the storage and peaking capacitors are 2nF. The spark gap is initially assumed to have a resistance R_1=0.1Ω and inductance L_1=2.2μF. The lengths of the discharge electrodes are 70cm and their widths are 1cm. The electrodes are separated with a gap of 1.0cm. The simulation is carried out at a gas pressure at 50mbar.

After the spark gap was triggered, the oscillation profile of the storage capacitor can clearly be seen due to the LCR discharge characteristics. The storage capacitor will transfer the charges to the peaking capacitor.

The peaking capacitor is being charged up to a critical level when the condition inside the discharge channel becomes ready for a breakdown to occur. The number density of the electron is increasing from the Townsend ionization process and the results are shown at Fig (4.3f). The initial value of 10^3 will then reach 10^{13} after the breakdown. From Fig (4.3b), the breakdown process happened at nearly 54nsec and the peaking capacitor will start to transfer all the energy or charges into the discharge channel. The voltage V_2 will decrease and the breakdown in the discharge gap occur.

By this time, the discharge current I_2 is increasing. The current profile is shown in Fig (4.3d). This current will reach the peak at nearly 1.35kA at 80nsec. Since the electrical discharge is fast, the peak current that is being produced is much higher when compared with current I_1, and the pulse width is almost 30nsec.

The gap resistance corresponding to the discharge is also shown in Fig (4.3e). The gap resistance at the discharge gap was in terms of Giga ohm and it will be reduced to less than one ohm after breakdown in a short period of time. By that time, the discharge channel is fully conductive.

For comparison purpose, Fig(4.3a) and Fig(4.3b) show the voltage profile generated by the new model and the Fitzsimmons's model. The results from these two models are expected to be identical even though they are computed using different algorithms. Both results show the identical breakdown voltage at about 54nsec. By that time, the discharge currents for both models as shown in Fig(4.3c) and Fig(4.3d) respectively are increased with a same profile until reaching the peak at about 83nsec. The peak values simulated by these models are identical with an error difference of less than 0.0005%.

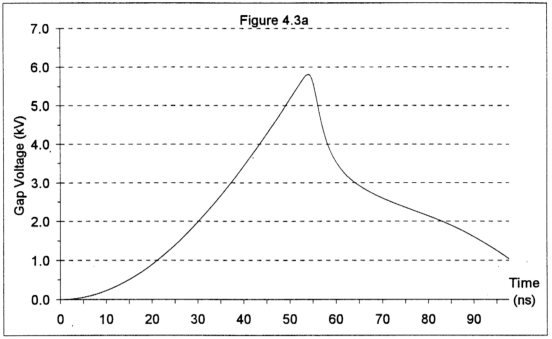

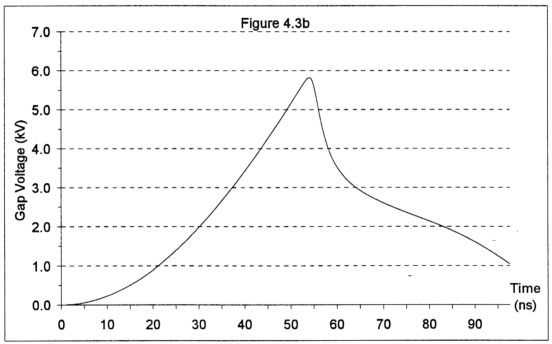

Figure 4.3: The Time-Dependent Gap Voltage; With Pressure p = 50mbar, Charging Voltage Vo = 20kV; With (a) Fitzsimmons's Model (b) The New Model With Uniform Electrical Field.

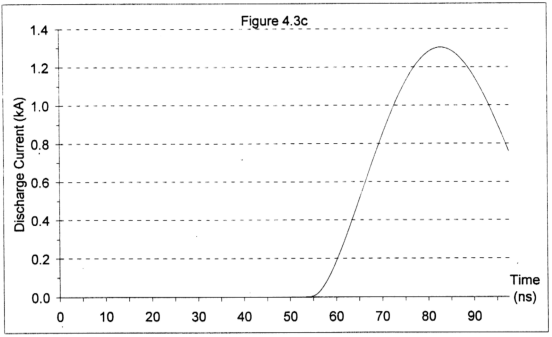

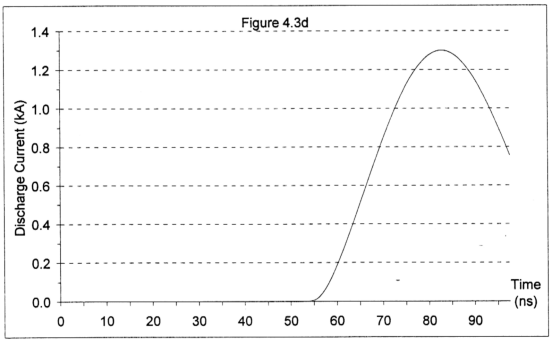

Figure 4.3: The Time-Dependent Discharge Current; With Pressure p = 50mbar, Charging Voltage Vo = 20kV; With (a) Fitzsimmons's Model (b) The New Model With Uniform Electrical Field.

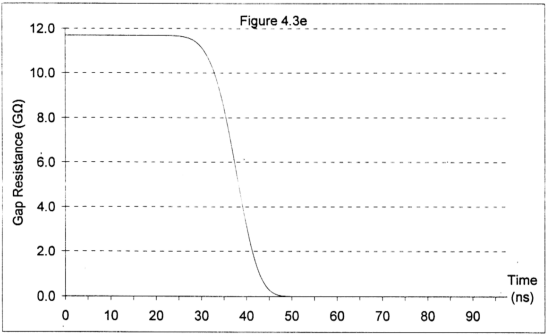

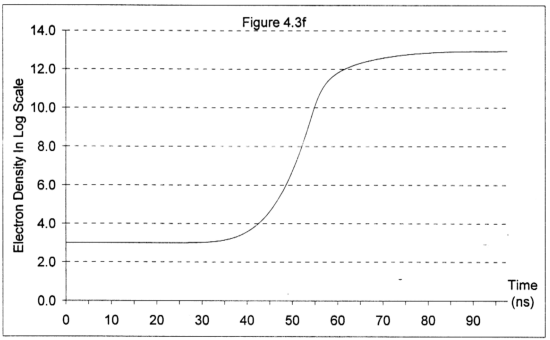

Figure 4.3:The Time-Dependent (e) Gap Resistance; and (f) Electron Densities That Generated By The New Model With Uniform Electrical Field.

From these results, we can conclude that the new model is able to reproduce the results as in Fitzsimmons's model even though a different computation algorithm is used.

4.4 THE STUDY OF NON-UNIFORM ELECTRICAL FIELD

In the previous section, the simulation was carried out by assuming the local electrical field and the charged carriers were uniformly distributed. However, these models are not the best models to describe the discharge. In the real discharge, the space charge effect and the secondary emission properties play important roles also. The information of the electron distribution and the cathode sheath formation will lead to further understanding of the behavior of the discharge.

For these reasons, the computational simulation of the fast electrical discharge needs to be carried out by using a non-uniform electrical field model. The electrical field variation can be calculated by the Poisson's equation and the motion of the charged particle can be easily simulated with the fluid equation.

4.4.1 THE DISTRIBUTION OF THE CHARGE CARRIERS AND THE LOCAL ELECTRICAL FIELD VARIATION UNDER THE SPACE CHARGE EFFECT

The basic idea of the non-uniform electrical field is due to the unequal distribution of the charge densities in the channel. In this study, the positive charge carrier is the N_2^+ ion and the negative charge carrier is the electron. In order to simplify the simulation of the cathode sheath, secondary emission effect at the cathode is neglected.

From the simulation of the computer model, the distribution of these charge carriers are shown in Fig(4.4.1) for a few selected times. At the beginning of the discharge process, the charge carriers with the same number densities are distributed uniformly in the discharge channel. When the external voltage from the electrical circuit is applied to the

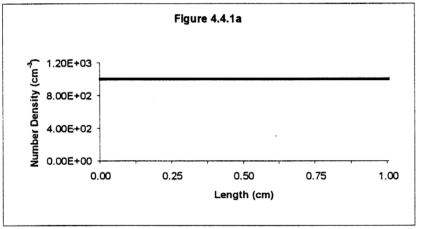

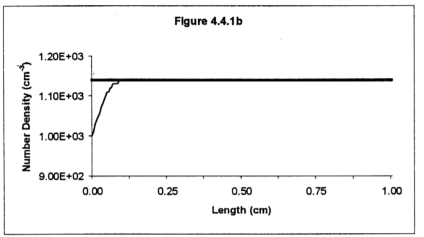

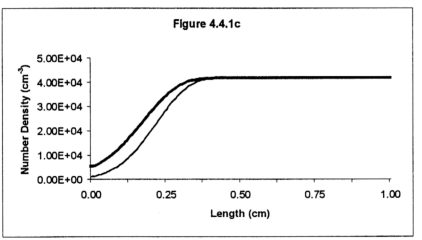

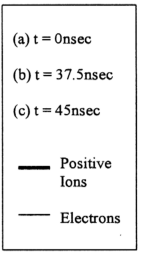

Figure 4.4.1: The Ion And Electron Density Distributions At Different Times.
(Same Conditions As In Figure 4.3)

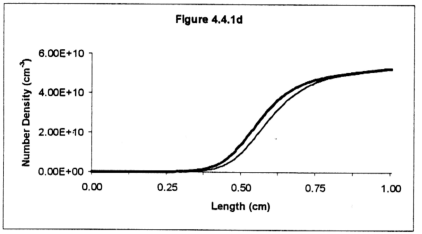

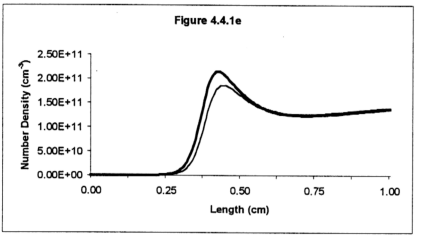

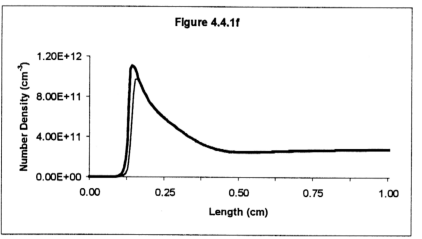

(d) t = 56nsec

(e) t = 58nsec

(f) t = 60.5nsec

Positive Ions

Electrons

Figure 4.4.1: The Ion And Electron Density Distributions At Different Times.
(Same Conditions As In Figure 4.3)

discharge gap, both the ions and electrons will be accelerated and move in the opposite directions. However, the different mobility due to the mass difference between these carriers will cause them to move with different velocities. The ions are relatively slow and looked like frozen in space when compared with the electrons.

From Fig (4.4.1b), during the time of 37.5nsec after the discharge, the non-uniform distribution of the electrons is clearly seen at the anode. The streamer formation process has started. Superposition of these streamers will lead to the formation of a space charge layer near the cathode. Furthermore, the cathode itself will only be emitting electrons under secondary effects, such as due to ion bombardment process.

This process will result in a non-zero diffusion term in the fluid equation near the cathode. Accumulation of this effect will lead to the formation of the space charge layer. However, the space charge effect is still not significant enough to cause a distortion of the local electrical field. At this time, the electrical field still looks like the uniformly distributed case as shown in Fig(4.4.1g).

The process above will keep going on and the Townsend ionization process is also on their way to create more pairs of charges due to ionization. Basically, the total number of both types of charges is also increasing with time. However, the rate of increase is likely to be slower at the region near the cathode. This is because of the drifting of the electrons is greater here due to the space charge effect. The densities of the charges have been clearly shown in Fig(4.4.1c) and Fig(4.4.1d). The positive column near the anode will have higher number charge densities, and the space near to the cathode still remain in low values due to the negative diffusion factor. However, the net charge density is still clearly seen where the ions with the low mobility are always left behind.

This process will continue until the discharge time of about 58nsec when the net charge density has become a significant number as shown in Fig(4.4.1e). The space charge

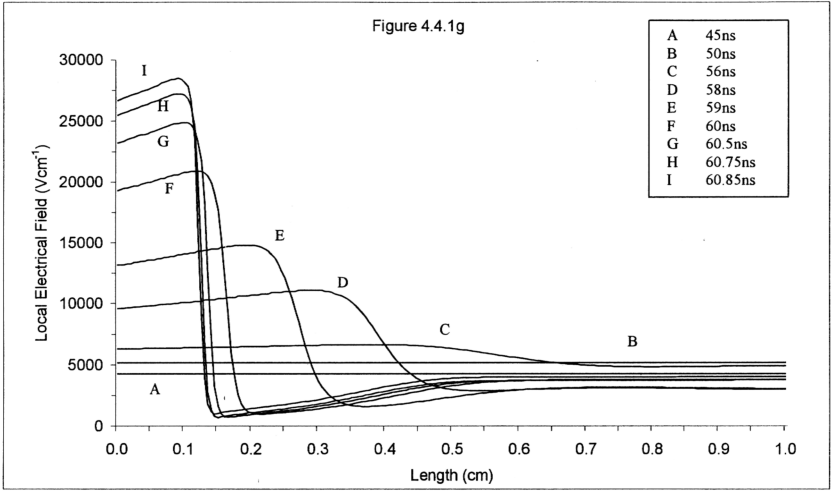

Figure 4.4.1g: The Electrical Field Distribution In The Discharge Channel Without Secondary Emission.

effect is large enough to influence the local electrical field distribution. The distortion of this electrical field profile can clearly be seen in Fig(4.4.1g). By this time, the electrical field in the discharge channel is no more in uniform distribution. From the Poisson equation calculation, the electrical field near the cathode will be higher when compared to the positive column near the anode. This effect will reduce the Townsend ionization process to a lower rate at the positive column when compared to the other mesh points along the channel. Finally, the medium will be separated into two zones. The first zone is the plasma region where the low field value is distributed homogeneously. The second is the high field plateau zone located at about one or two millimeters from the cathode.

However, the high local electrical field at the space near the cathode will then speed up charges. Although the Townsend ionization process is taking place, the larger diffusion term will still move the charges away due to the high value of local electrical field.

Finally, the increase in the number densities can be seen in the middle of these two regions. In this region, the densities of the charges is accumulating since the positive column which has a lower local electrical field will become the 'bottle neck' and blocks the further motion of the electrons. The formation of the charges finally ended at the region near to the cathode due to the equivalent condition of the Townsend ionization and the diffusion processes. A clear layer which is almost empty of charges is formed near to the cathode, and this layer is called the cathode sheath.

The cathode sheath length is defined as the distance between the cathode and the point in the cathode region at which the electron density becomes larger than the ion density. From Fig(4.4.1g), the length of the layer is almost 1.2mm away from the cathode. At this stage, the current of the discharge loop is still a low value.

4.4.2 THE IMPORTANT ROLE OF THE ION BOMBARDMENT PROCESS AS THE SECONDARY EMISSION EFFECT IN THE BREAKDOWN PROCESS

The cathode sheath appears to be like a capacitor where charges are being held. However, in the real case, the length of the cathode sheath may not be so clearly defined because there is also a contribution of the secondary electrons emitting from the surface of the cathode. The introduction of a secondary emission process into the present model allows one to obtain a realistic cathode region structure and also the sheath formation and evolution as shown in Fig(4.4.2a).

There are a few mechanisms of creating secondary emission electrons. However, only the ion bombardment process will be taken into consideration in this study, since it is the major contributor to the secondary effects (Fletcher, 1981). This process is taking place when the local electrical field at the cathode reaches a critical level. The high local electrical field will create high velocity ions. The ions may get enough energy to release the electrons from the cathode through bombardment processes (Fletcher, 1981; Spyrou, 1991).

The contribution of these secondary properties will play a significant role in the breakdown process. The beginning of the breakdown process happened when the number of electrons emitted is large enough to move the positive net charge density in the cathode region. These secondary electrons will act like the linkage capacitor resulting in the cathode sheath being successively destroyed in the cathode region.

The clear evolution of the local electrical field is shown in Fig(4.4.2a). For the first 50nsec, the electrical field is still uniformly distributed. The distortion of the local electrical field is clearly seen after 56nsec. Within a short period, the local electrical field at the cathode reaches more than 10kV/cm. The process of cathode sheath formation until its collapse takes about 4 to 5 nanoseconds.

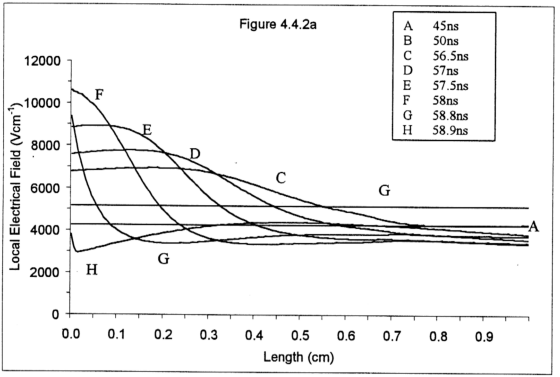

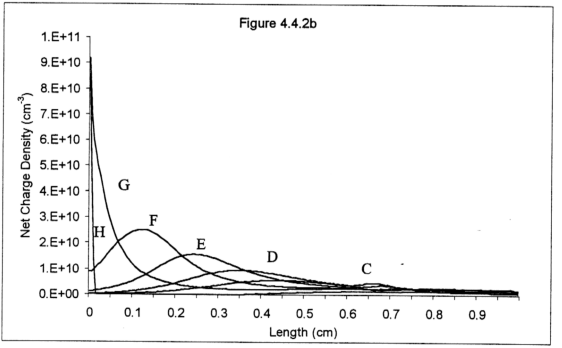

Figure 4.4.2: (a) The Local Electrical Field Distribution; (b) Positive Net Charge Density, In The Discharge Channel. (Same Condition As In Figure4.3)

The corresponding positive net charge densities are also shown in Fig(4.4.2b). From these results, the collapsing of the net charges is likely to be seen at 59nsec.

This cathode sheath also behaves as a natural switch to turn on the electron avalanche in the discharge channel.

Fig(4.4.2f) shows the results of the reaction of the electron density at the cathode with the time evolution. The avalanche effect can be seen at about 59nsec where the number density increases by a few orders of magnitude in a short period of time (less than 1nsec). The corresponding results are also shown in Fig(4.4.2c) to Fig(4.4.2e) for the time-dependent voltage profile with a 'hump' at that particular time, expressing the electron avalanche and also the collapsing of the positive net charge density. The computer model manages to simulate the same profile accurately although different mesh sizes of 0.0025cm, 0.004cm and 0.005cm had been used. During this very short phase, the ion population of the cathode is sufficiently large to cause the creation of secondary electrons, which contributes to the electron current amplification. By this time, the discharge current has distinctly increased as shown in Fig(4.4.2g).

During the time where the net charge density collapses, the cathode sheath will disappear. The whole discharge gap becomes fully conductive and the breakdown process has completely occurred. The charge densities will increase almost uniformly. The whole process will lead to an increase of the current in the discharge channel, and can be calculated by the Sato's equation.

This result is different with a uniform electrical field model. The previous model emphasized on the accumulation of number charge carriers via the Townsend ionization process. The large number of charges will reduce the dynamic resistance of the discharge gap until a critical level, then the breakdown process takes place. This previous model is

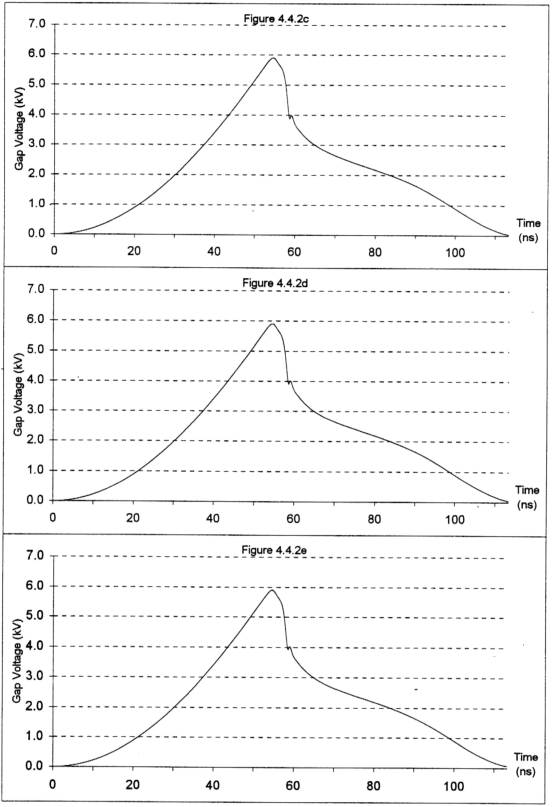

Figure 4.4.2: Voltage Across The Discharge Gap; Simulation With Different Mesh Sizes. (c) $\Delta x = 0.0025$cm; (d) $\Delta x = 0.004$cm; (e) $\Delta x = 0.005$cm.

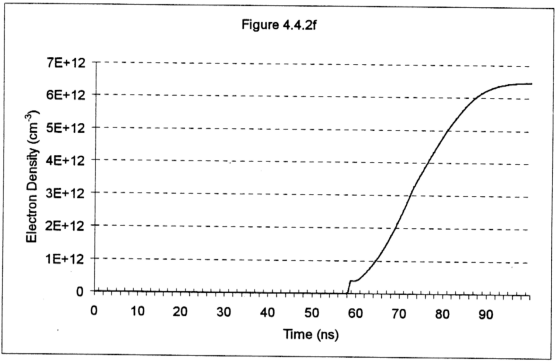

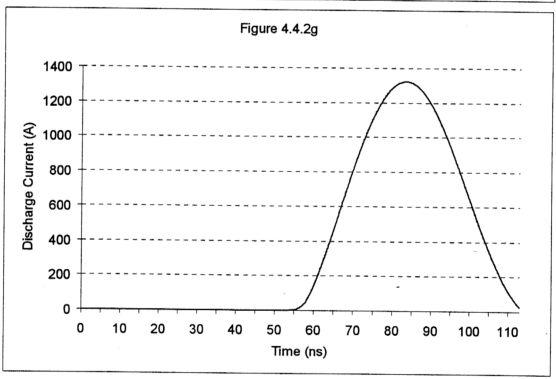

Figure 4.4.2: (f) Electrons Density At The Surface Of The Cathode. (g) The Discharge Current. (Same Condition As In Figure 4.3)

not able to describe the breakdown and avalanche processes and also the roles played by the secondary emission at the cathode.

4.4.3 THE SPACE CHARGE EFFECTS AND THE ELECTRICAL DISCHARGE CHARACTERISTICS

In this section, the space charge effects and its influences on the electrical discharge characteristics will be studied and discussed.

Fig(4.4.3a) and Fig(4.4.3b) show the results of electrical discharge voltage of the laser channel. Both cases of uniform and non-uniform electrical field are studied here. For the case of non-uniform electrical field, the space charge effect is included into the simulation. However, the space charge effect is ignored if simulation is done with uniform electrical field.

From the results, both cases show the same profiles of increasing in the gap voltage at the beginning of the discharge. However, the discharge which is simulated by the non-uniform electrical field will take a longer time to breakdown and also a higher breakdown voltage at about 5.90kV. This is different from the case for uniform electrical field where the breakdown voltage is lower at about 5.82kV and this happens at 1 to 2 nanoseconds earlier. These differences on the both cases are due to the space charge effect which has been taken into consideration in the non-uniform electrical field model.

The behavior of the space charge has been studied in the previous section. This layer of space charge will be able to hold the charges before the breakdown process occurs. This natural behavior of the space charge will delay the breakdown. This layer would also allow the breakdown to occur at a higher breakdown voltage. However, this effect is always neglected if the uniform electrical field has been used.

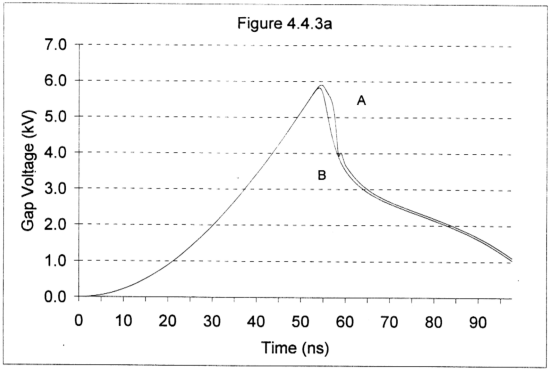

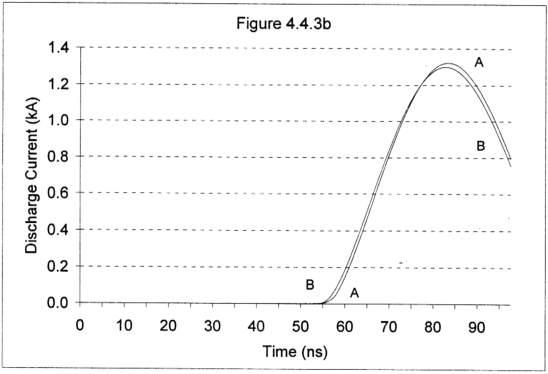

Figure 4.4.3: Comparison Of Two Different Simulation Model On
(a) Gap Voltage; (b) Discharge Current (Same Condition As In Figure 4.3)

A = Non Uniform Electrical Field
B = Uniform Electrical Field

The same condition can also be shown at the discharge current profile. Fig(4.4.3b) shows the results of the discharge current under the uniform and non-uniform electrical field. For the case of non-uniform electrical field, a significant increase in the discharge current is expected at 1 to 2 nanoseconds slower when compared with the case of uniform electrical field. However, this discharge current is able to reach a higher peak current at 1.32kA, compared to 1.30kA where the simulation is done without the space charge effect. This is because of the avalanche effect where the positive net charge density collapses at the surface of the cathode. This avalanche effect will efficiently reduce the FWHM of the discharge current and a higher peak current will be achieved.

This shows the important role of the space charge effect which contributes to the electrical discharge. This space charge effect will further explain on the discharge behavior which is always unable to be explained by the uniform electrical discharge model.

4.5 THE INFLUENCE OF THE EXTERNAL ELECTRICAL DISCHARGE CIRCUIT

Some important electrical circuit parameters play important roles in the breakdown process occurring in the discharge gap. These parameters are expected to affect the electrical energy transfer process during the discharge.

4.5.1 THE SPARK GAP PROPERTIES.

In this section, the spark gap properties and its influences on the space charge effect will be studied. Simulation is carried out at varying initial spark gap inductances of 2.2μH, 5μH and 10μH. The results are shown in Fig(4.5.1).

The voltage rise time is proportional to the inductance of the spark gap. From the results, it can clearly be seen that the larger value of the inductance will cause poor

electrical discharge properties. The large value of inductance will slow down the energy transfer process and reduced the efficiency as a fast electrical discharge circuit for laser applications.

From the Fig(4.5.1a), the voltage risetime is almost 106.1nsec if the spark gap's inductance is 10μH. However, the voltage risetime can be reduced down to 54.6nsec if spark gap has a lower inductance of 2.2μH.

Only the lower inductance will efficiently transfer charges from the storage capacitor to the peaking capacitor and finally to the discharge channel. From the Fig(4.5.1a), the results for 2.2μH will have the maximum energy transfer at higher breakdown voltage of 5.9kV, when compared with the case of 10μH which can just reach 4.9kV, even though both cases have the same charging voltage.

The fast discharge with lower inductance creates an efficient secondary emission process. From Fig(4.5.1c), the results show the number density of electrons at the cathode under these three conditions. Only the fast discharge will be able to create a large population of secondary electrons at an earlier time. This population is significant to create the electron avalanche effect and subsequently reach a higher peak discharge current as shown in Fig(4.5.1b).

The advantages of the lower inductance can be seen by the space charge formed. Once the discharge occurs with a shorter risetime, space charge effect and the positive net charge density is much more significant as shown in Fig(4.5.1c). The local electrical field at the cathode is correspondingly higher. Results from Fig(4.5.1d) show that the local electrical field might reach about $11kVcm^{-1}$ when low inductance of 2.2μH is initially assumed, in contrast with about $9kVcm^{-1}$ when high inductance of 10μH.

The net charge density profile at Fig(4.5.1g) also shows the greatest value of positive net charges when the cathode sheath collapses at the surface of the cathode. This

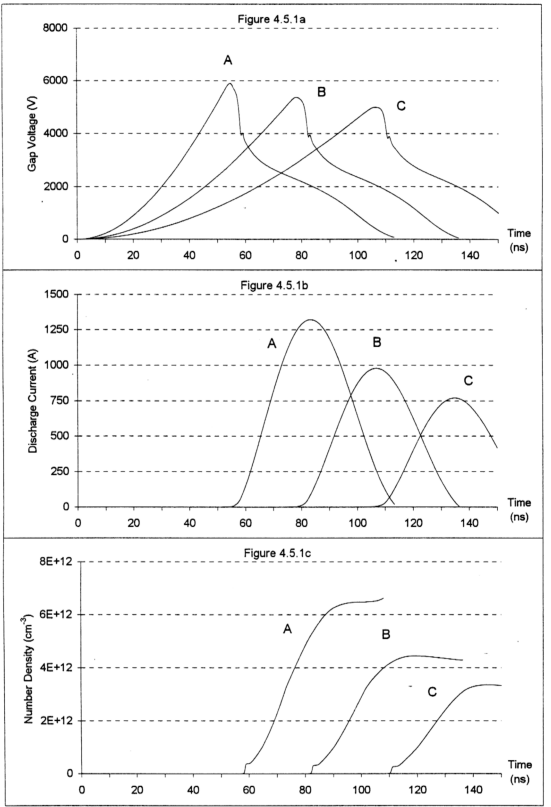

Figure 4.5.1: (a) Gap Voltage; (b) Discharge Current; (c) Electron Density at the cathode; Inductance Of Spark Gap, A. 2.2μH, B. 5μH, C. 10μH.

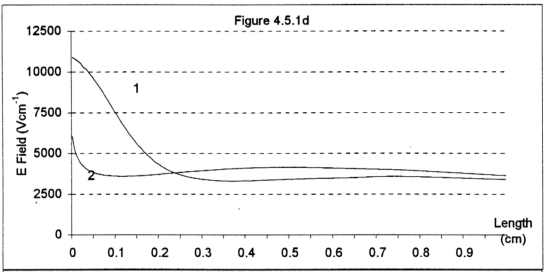

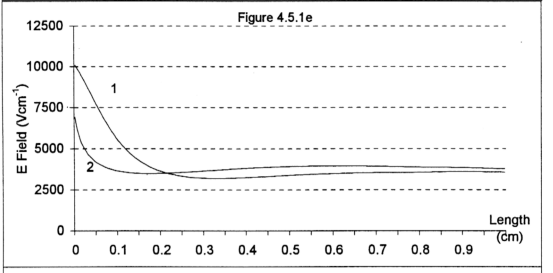

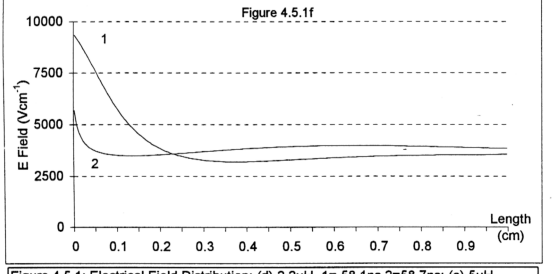

Figure 4.5.1: Electrical Field Distribution; (d) 2.2μH, 1= 58.1ns 2=58.7ns; (e) 5μH, 1=82.2ns 2=82.6ns; (f) 10μH, 1=110.0ns 2=110.4ns.

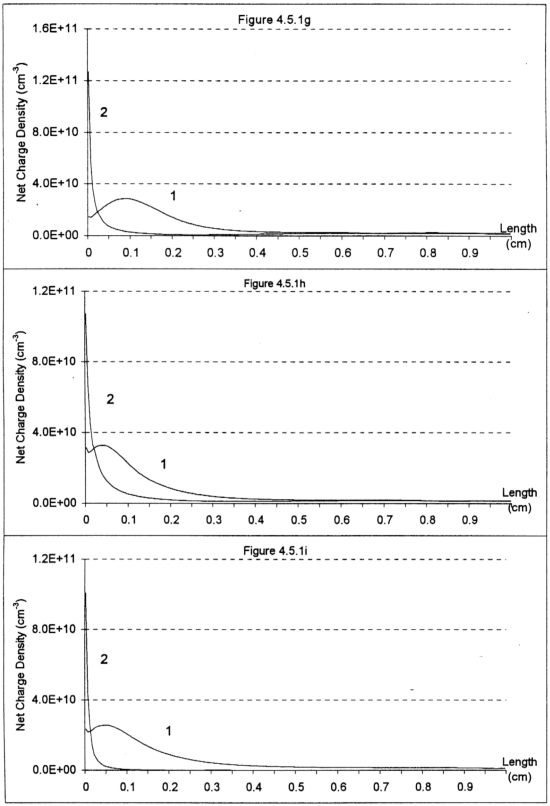

Figure 4.5.1: The Positive Net Charge Density Distribution; (g) 2.2μH, 1=58.1ns, 2=58.7ns; (h) 5μH, 1=82.2ns, 2=82.6ns; (i) 10μH, 1=110.0ns, 2=110.4ns.

condition enables greater ion bombardment process to occur when compared to the cases of 5μH and 10μH as shown in Fig(4.5.1h) and Fig(4.5.1i). A large number of the electrons will be released from the surface of the cathode and contribute to the ionization process. The total electron current generated is large and resulting in the high peak current at 1.32kA. Overall performance will thus be affected if the inductance is getting larger.

4.6 THE INFLUENCE OF GAS PRESSURE

In this section, the influence of the gas pressure on the electrical discharge will be studied. Simulation has been carried out with three different operating gas pressures of 30mbar, 50mbar and 70mbar.

Basically, the higher pressure will lead to the lower mobility of the charge carriers. Amplification of the charge carriers through Townsend ionization process is slower. This will cause the breakdown of the discharge gap to take a longer charging time. Finally, it will lead to a longer risetime of the discharge voltage.

However, the low mobility of the particles may create a more significant space charge effect in the discharge channel. The maximum local electrical field at the cathode may reach 7.2kVcm^{-1} during the collapsing of the net charge density, at a gas pressure of 70mbar. This condition finally leads to a significant secondary emission process and a large number of secondary electrons will be released from the cathode. Finally, the discharge may still remain at a higher peak current.

From the results at Fig(4.6a), the highest breakdown voltage that can be achieved is 7.2kV when a higher gas pressure of 70mbar is applied. The decrease in the breakdown voltage can be seen when the gas pressure is reduced.

As expected, the peak of the discharge current as shown in Fig(4.6b) increases if higher pressure is applied, reaching a maximum peak at the gas pressure of 70mbar.

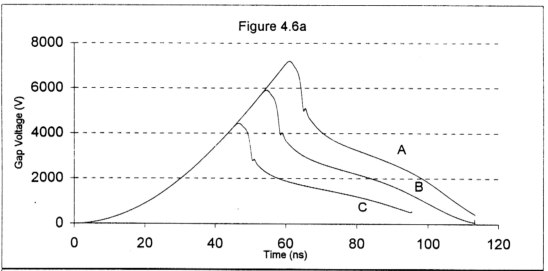

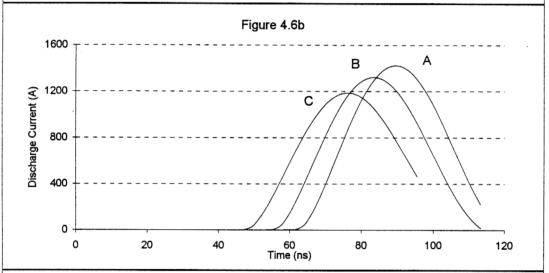

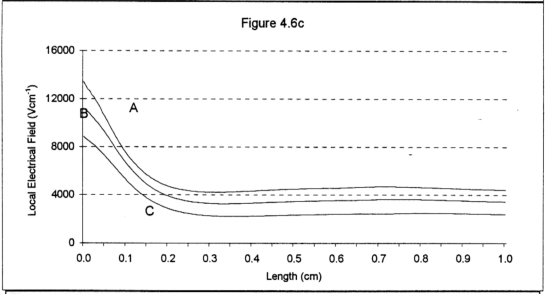

Figure 4.6: (a) Gap Voltage; (b) Discharge Current; (c) E Field Distribution
Pressure A. 70mbar; B. 50mbar; C. 30mbar

Fig(4.6c) show the results of the electrical field distribution in the discharge channel. If a higher pressure has been applied, the maximum local electrical field at cathode is generally higher by the time the cathode sheath is collapsing.